

DOI: 10.1002/cbic.200800249

Isofagomine Induced Stabilization of Glucocerebrosidase

Gregory J. Kornhaber,^[a] Michael B. Tropak,^[b] Gustavo H. Maegawa,^[b] Steven J. Tuske,^[a] Stephen J. Coales,^[a] Don J. Mahuran,^[b, c] and Yoshitomo Hamuro^{*[a]}

Structurally destabilizing mutations in acid β -glucosidase (GCase) can result in Gaucher disease (GD). The iminosugar isofagomine (IFG), a competitive inhibitor and a potential pharmacological chaperone of GCase, is currently undergoing clinical evaluation for the treatment of GD. An X-ray crystallographic study of the GCase-IFG complex revealed a hydrogen bonding network between IFG and certain active site residues. It was suggested that this network may translate into greater global stability. Here it is demonstrated that IFG does increase the global stability of wild-

type GCase, shifting its melting curve by $\sim 15^\circ\text{C}$ and that it enhances mutant GCase activity in pre-treated N370S/N370S and F213I/L444P patient fibroblasts. Additionally, amide hydrogen/deuterium exchange mass spectroscopy (H/D-Ex) was employed to identify regions within GCase that undergo stabilization upon IFG-binding. H/D-Ex data indicate that the binding of IFG not only restricts the local protein dynamics of the active site, but also propagates this effect into surrounding regions.

Distended macrophages, the hallmark feature of Gaucher disease (GD), arise due to the massive accumulation of the glycolipid, glucosylceramide (GC) in lysosomes. GD has been linked to certain mutations in GBA, the gene encoding the enzyme glucocerebrosidase (GCase), that negatively affect the ability of GCase to convert lysosomal GC to D-glucose and ceramide. The effects of GC accumulation extend downstream of the lysosome,^[1] resulting in altered calcium homeostasis and phospholipid synthesis; this can lead to endoplasmic reticulum stress and/or inflammatory responses. Either of these responses can effect cellular growth and trigger apoptosis.^[2] This disorder is characterized by an enlarged liver and spleen, anemia, painful bone lesions and in some cases neurological damage. The standard treatment for individuals with GCase deficiencies involves either enzyme replacement therapy with imiglucerase (Cerezyme, Genzyme Corp.)^[3] or less frequently, substrate reduction therapy with miglustat (Zavesca, Actelion Ltd.)^[4,5] Recently a third therapeutic approach, enzyme enhancement therapy (EET), utilizing small molecule pharmacological chaperone (PC) has been proposed. Currently, isofagomine (IFG), an iminosugar and potent competitive inhibitor of GCase (Plicera, Amicus Therapeutics Inc.) is being evaluated clinically as a PC for EET.^[6-8]


IFG, like other GCase PCs, is a competitive inhibitor with IC_{50} values of 5 and 30 nM at pH 7.2 and pH 5.2, respectively.^[8] Surprisingly, it has been shown to be effective as a PC in cultured patient cells only at concentrations significantly higher than its IC_{50} , 10–100 μM .^[8] This likely reflects the fact that the efficacy of a PC not only depends on its affinity for the target enzyme but also on its bioavailability in terms of membrane permeability, subcellular distribution and metabolism.^[9] Thus, the actual intracellular concentration of IFG after treatment is likely much less than the extracellular concentration. The actual concentration and any residual inhibitory effects IFG might have on lysosomal GCase are difficult to determine, as the *in vitro* assays for GCase enhancement include washing of cells prior to lysis and dilution of the intracellular IFG by the addition of lysis and assay buffers (> 100-fold).

Among Caucasians, N370S has been identified as the most common GD associated missense mutation; 75% of GD patients of Ashkenazi Jewish descent harbor at least one allele encoding this substitution.^[10,11] Among the Asian population, L444P (Type II, neurological) and F213I (Type I) have been identified as the first and second most frequent mutations. N370S is associated with impaired intracellular trafficking resulting in a reduction in lysosomal concentrations of GCase.^[12,13] Due to the possible destabilizing effect of the N370S substitution, the folding rate of GCase in the endoplasmic reticulum (ER) is believed to be decreased, thus allowing the ER-associated degradation machinery (ERAD) time to recognize and redirect the unfolded protein to the cytosolic proteasome.^[14,15] Cell-based activity and immunofluorescence assays have demonstrated an IFG-dependent increase in lysosomal pools of enzymatically active N370S GCase.^[7,8,16] Steet et al.^[8] proposed that IFG increases the exit of mutant GCase from the ER. Given that the kinetic properties of the mutant enzyme following treatment with IFG resembled those of the wild type enzyme, it was further proposed that the increased ER export occurred because of the stabilization of natively folded N370S GCase, which was induced by the formation of IFG-GCase complexes. This proposal is consistent with the previously published FOLDEX model of protein folding and/or degradation within the ER.^[17]

[a] Dr. G. J. Kornhaber, Dr. S. J. Tuske, S. J. Coales, Dr. Y. Hamuro
ExSAR Corporation
11 Deer Park Drive, Suite 103, Monmouth Junction, NJ 08852 (USA)
Fax: (+1) 732-438-1919
E-mail: yhamuro@exsar.com

[b] Dr. M. B. Tropak, Dr. G. H. Maegawa, Prof. Dr. D. J. Mahuran
Research Institute, Hospital for Sick Children
555 University Avenue, Toronto, ON M5G 1X8 (Canada)

[c] Prof. Dr. D. J. Mahuran
Laboratory of Medicine and Pathobiology, University of Toronto
Banting Institute, 100 College Street, Toronto, ON M5G 1L5 (Canada)

 Supporting information for this article is available on the WWW under <http://www.chembiochem.org> or from the author.

In recent X-ray crystallographic studies Lieberman et al.^[7] identified an extensive hydrogen bonding network between IFG and six GCCase active site residues. This network stabilized a particular active site conformation that the authors suggested promoted greater global stability.^[7] Here we probe the effects of IFG-binding in solution on GCCase global stability by differential scanning fluorimetry^[18–22] and on local dynamics by amide hydrogen/deuterium exchange coupled with proteolysis and mass spectrometry (H/D-Ex).^[23–28] The ability to partially restore intracellular trafficking and lysosomal GCCase localization of mutant forms of GCCase was then inferred from activity assays performed on N370S/N370S and F213I/L444P patient fibroblasts. These experiments were employed to gain a better understanding of the PC mechanism associated with IFG binding, particularly the relationship between local dynamics, global stability in solution and their effect on lysosomal concentrations of the enzyme.

Results

IFG enhances global stability and activity

The thermal stability of GCCase (Cerezyme) in the absence and presence of increasing concentrations of IFG was determined using differential scanning fluorimetry (DSF) by monitoring the increase in emission intensity of NanoOrange,^[18–20,29] an environmentally sensitive fluorescent probe that undergoes fluorescence enhancement upon exposure to the hydrophobic interior of a protein. As the temperature is elevated, the fluorescence intensity of NanoOrange increases as a larger proportion of the GCCase in solution unfolds, enabling binding of the probe to the hydrophobic interior. As shown in the inset in Figure 1A, the melting temperature (T_m) of GCCase is defined as the midpoint in the thermal ramp from the period when the fluorescence intensity increases until peak intensity. This value represents the transition point in the equilibrium between the folded and non-native states of the protein. At the maximum concentration of IFG evaluated (43 μM), the T_m of wild-type GCCase in the presence of the ligand was increased by approximately 15 °C relative to the T_m (49 °C) observed for GCCase in the absence of IFG (see Figure 1B).

Previous measures of N370S GCCase activity of fibroblasts pretreated with increasing concentrations of IFG, identified a maximum dose response at ~30 μM IFG.^[7] Two GD patient fibroblast cell lines, one harboring N370S/N370S and the other F213I/L444P GCCase mutations, were treated with IFG for five days and intracellular GCCase activity following lysis of cells was determined with the aid of the artificial substrate 4-methylumbelliferyl-beta-D-glucopyranoside (MUGlc).^[30,31] An increase in enzymatic activity is observed as an increase in fluorescence upon release of the 4-methylumbelliferyl fluorophore. Treatment of N370S/N370S and F213I/L444P fibroblasts with 25 μM IFG for five days enhanced GCCase activity 2.5- and 4.3-fold over non-pretreated cells, respectively (see Figure 1C). The increased activity of the F213I mutation extends the panel of GCCase mutations (N370S^[8] and G202R^[9]) whose activity can be enhanced by IFG.

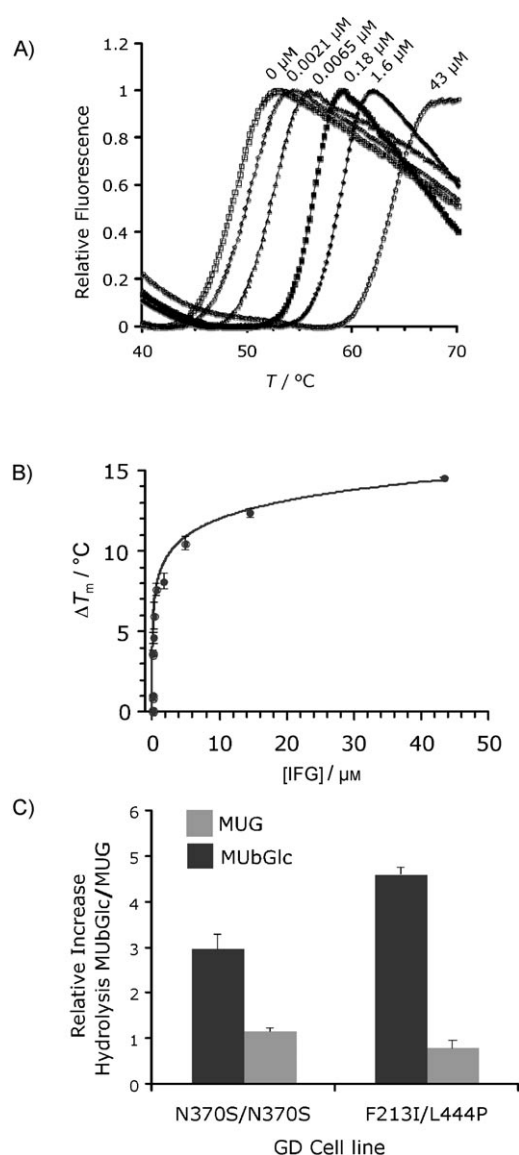


Figure 1. The impact of isofagomine (IFG) on GCCase stability and activity. A) Thermostability of GCCase in the absence and presence of increasing concentrations of IFG as measured by differential scanning fluorimetry (DSF). Unfolding of GCCase was monitored by the change in relative fluorescence levels of the fluorophore NanoOrange with increasing temperature. B) Increase in T_m relative to ligand-free GCCase (ΔT_m (°C) = T_m [IFG] – T_m [DMSO]) in response to increasing concentrations of IFG ($n=2$). C) Relative increase in GCCase activity (Black Box) as a result of IFG treatment. Cell lines derived from GD patient fibroblasts carrying either N370S/N370S or F213I/L444P substitutions were treated with IFG (25 μM). Activity levels are relative to cells treated with dimethyl sulfoxide. β -Hexosaminidase (HEX) activity levels (gray bars) serve as an experimental control, as IFG does not inhibit HEX (data not shown) or affect its activity in treated cells ($n=2$).

H/D-Ex analysis of ligand-free GCCase

Purified GCCase (Cerezyme/Imiglucerase) in the presence or absence IFG was incubated in deuterated buffer (pH 7.8) for a predetermined period and proteolyzed by immobilized pepsin.^[32] Then the mass of each peptide was determined by liquid chromatography mass spectrometry (LC/MS). Deuteration levels of 61 GCCase peptides were determined at different

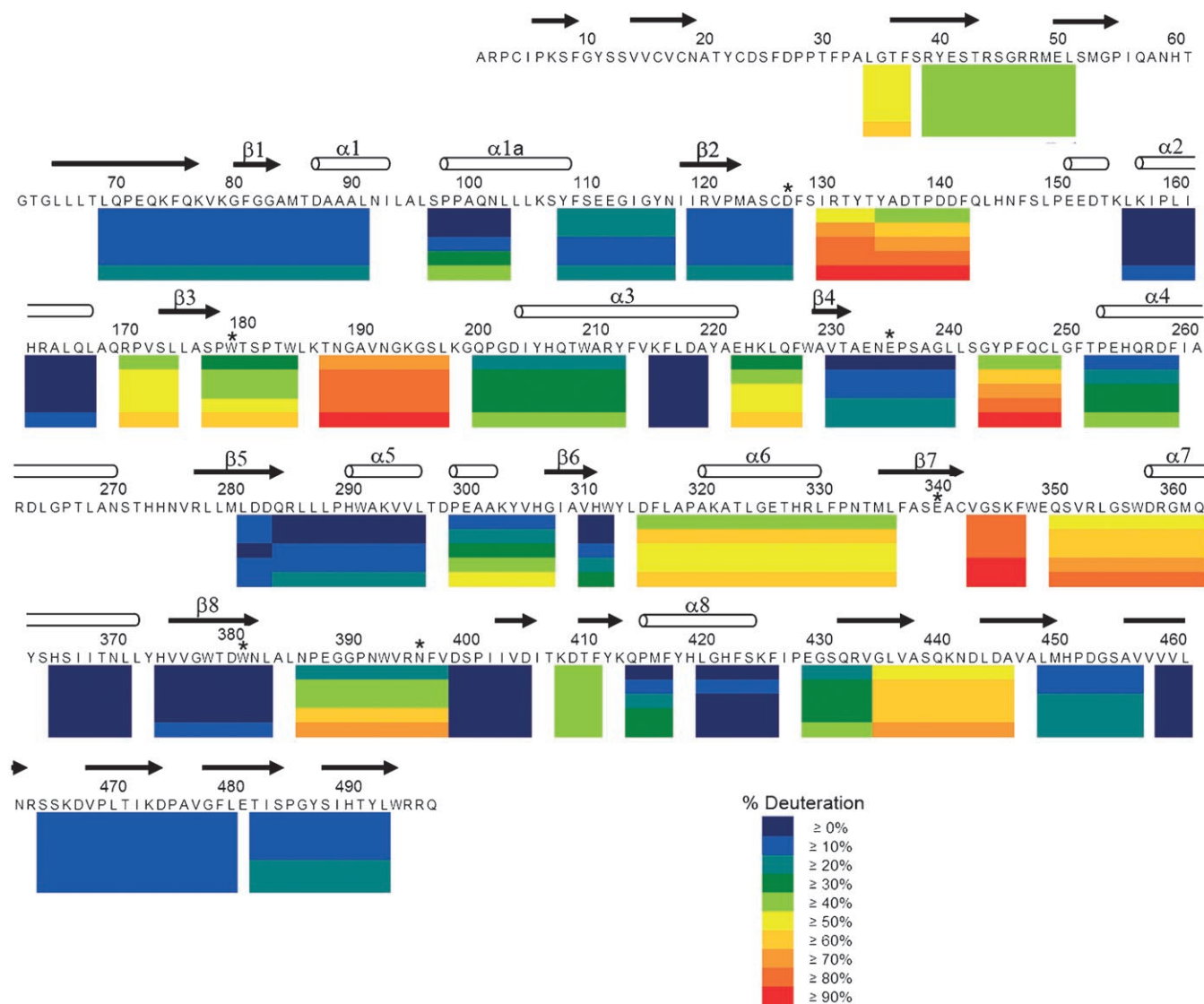


Figure 2. Deuteration level of peptides derived from different GCCase regions. The deuterium uptake over 30, 100, 300, 1000 and 3000 s (in descending order) is displayed below the sequence of GCCase according to the color code given in the legend, lower right. The secondary structure elements found in domain II (PDB ID: 2NSX) are denoted as symbols above the sequence. Residues forming hydrogen bonds with isofagomine (IFG) are denoted by asterisks. Position of residues corresponding to mutations G202R, F213I, N370S and L444P are boxed and outlined in red.

time points (see Figure S1 in the Supporting Information). These peptides cover 82% (408/497 residues) of the protein's sequence (Figure S2). Four of five missing regions contained a glycosylated asparagine residue of unknown mass, thus precluding LC/MS identification.

Only 35% of GCCase was deuterated under the conditions and time frame of analysis, indicating that it is a predominantly stable protein (Figures 2 and 3, Table S1). The fastest exchanging regions (deuterated $>60\%$ on average) were segments 130–134, 135–142, 187–197, 243–249, 343–347, 386–400, and 435–446. Loop regions (shown red or orange in Figure 3) comprised the most dynamic regions of GCCase. The most slowly exchanging regions (deuterated $<20\%$ on average) were segments 69–91 ($\beta 1$ and $\alpha 1$), 119–127 ($\beta 2$), 156–167 ($\alpha 2$), 215–219 ($\alpha 3$), 230–240 ($\beta 4$), 281–283 ($\beta 5$), 284–296 ($\alpha 5$), 310–312 ($\beta 6$), 365–371 ($\alpha 7$), 374–383 ($\beta 8$), 399–405 (β), 420–426 ($\alpha 8$), 449–

457 (β), 459–461 (β), 464–480 (β), and 482–493 (β). These rigid regions formed the most stable protein folding core of GCCase (shown blue in Figure 3).

IFG stabilization of loop, active site and internal regions

IFG addition resulted in strong negative perturbations ($\geq 9\%$ decrease in average deuteration level) in nine regions corresponding to segments 119–127, 177–184, 187–197, 230–240, 243–249, 310–312, 343–347, 386–400 and 414–417 (Figures 4 and 5, Table S2). A negative perturbation is the result of a reduction in the local unfolding rate of a particular region. The 6% drop observed in the average deuteration level of all segments is likely an indication of a net global stabilization upon IFG addition. No meaningful positive perturbations ($>5\%$ increase in average deuteration level) correlated with IFG addi-

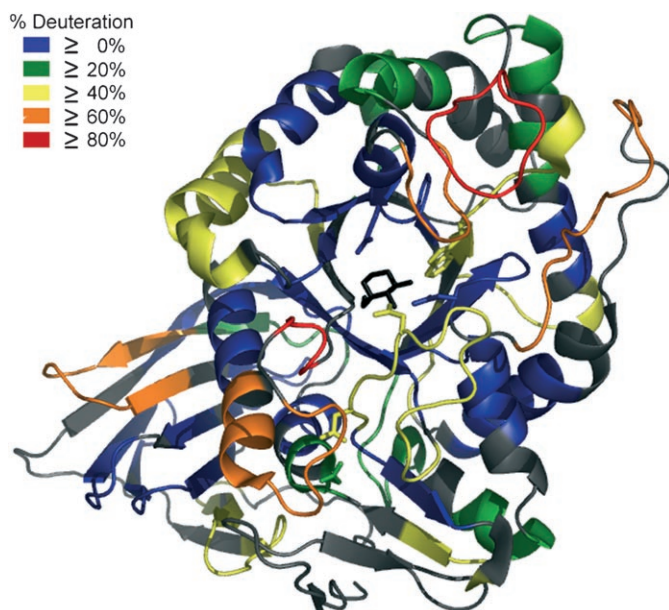


Figure 3. Color highlighted average deuterium level of each peptide superimposed upon the ribbon diagram representation of the GCCase X-ray crystal structure (PDB identifier 2NSX) bound to isofagomine (stick representation color red black). The average deuterium level of each peptide is color coded as shown at the bottom. Illustration generated with PyMOL (DeLano Scientific).

tion. Based on the 3D structure of the recently determined GCCase-IFG complex, residues Asp127, Trp179, Glu235 and Asn396, which form hydrogen bonds with IFG at the active site of the enzyme,^[7] were found to reside within four of the

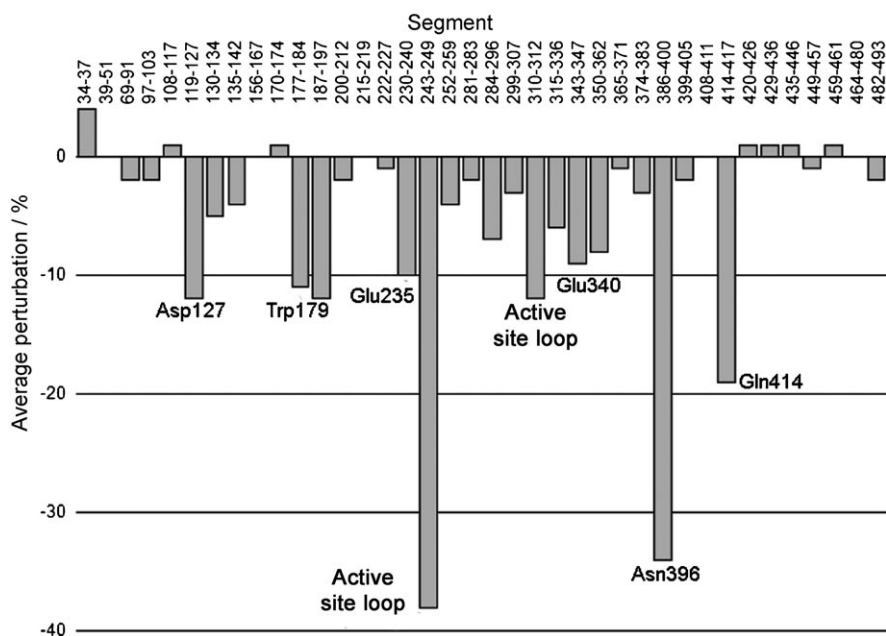


Figure 4. Changes in average deuterium incorporation (perturbations) of segments in response to isofagomine (IFG) binding. Positive perturbations are indicative of increased mobility, whereas negative values indicate structural rigidification. Labeled are columns for segments comprising the active site or including residues that form hydrogen bonds to IFG (Asp127, Trp179, Glu235, Glu340 and Asn396). Also indicated is Gln414, a residue residing in rigidified segment 414–417, which is likely hydrogen bonded to Asp399, a residue residing in stabilized segment 386–400.

regions showing strong perturbation (Figures 4 and 5; 119–127 (β 2), 177–184 (β 3), 230–240 (β 4), and 386–400 (loop)). Segment 343–347 resides in a loop region near Glu340, which is also hydrogen bonded to IFG. Perturbations at 187–197 (loop) and 243–249 (loop) correspond to adjacent loop regions at the mouth of the active site.

The perturbation observed in 310–312 (β 6) is likely due to overlap with loop 1 region (residues 311–319).^[7] At neutral pH and in the absence of ligand, loop 1 can assume two different conformations: helical turn and irregular secondary structure (PDB ID: 2NT1). In contrast to the neutral pH apo structures, loop 1 in the IFG bound GCCase structure (PDB ID: 2NSX) was observed solely in the helical turn conformation. On the basis of these observations it was proposed that in the absence of substrate or inhibitor, loop 1 undergoes dynamic sampling of the two conformational extremes, whereas in the presence of IFG, the conformation with the helical turn is stabilized. The present data have demonstrated the stabilization of loop 1 upon IFG binding, which is consistent with the earlier conclusion that IFG binding stabilizes one of two possible conformations known to be sampled by loop 1.^[7]

A strong perturbation was also observed in segment 414–417 (α 8), a region corresponding to a portion of helix α 8 of domain III (Figures 4 and 5; Table S2). This region does not lie in or around the active site, but instead abuts one of two β -sheets constituting domain II. The slower H/D exchange rate in this segment upon IFG-binding may result from a propagation of changes in the hydrogen bonding network involving residues Gln414 and Asp399, ultimately resulting in an increase in rigidification of this region. Residue Asp399 resides in the ligand stabilized segment 386–400 (loop), a region that includes Asn396, a residue directly hydrogen bonded to IFG at the active site. Although primarily surface accessible, segment 386–400 (loop) nonetheless includes a subset of solvent excluded residues. In this buried region Asp399 is likely hydrogen bonded to Gln414, given that the interatomic distance between Asp399-O δ and Gln414-N ϵ is 2.6 Å (PDB identifier 2NSX).

There are four segments that show intermediate perturbations (5–8% decrease in average deuteration level) upon IFG binding: 130–134, 284–296 (α 5) is conformationally adjacent to IFG hydrogen bonded residue Asp127. Segment 284–296 (α 5) is conformationally adjacent to region 310–312 (β 6). Segment 315–336 (α 6) is con-

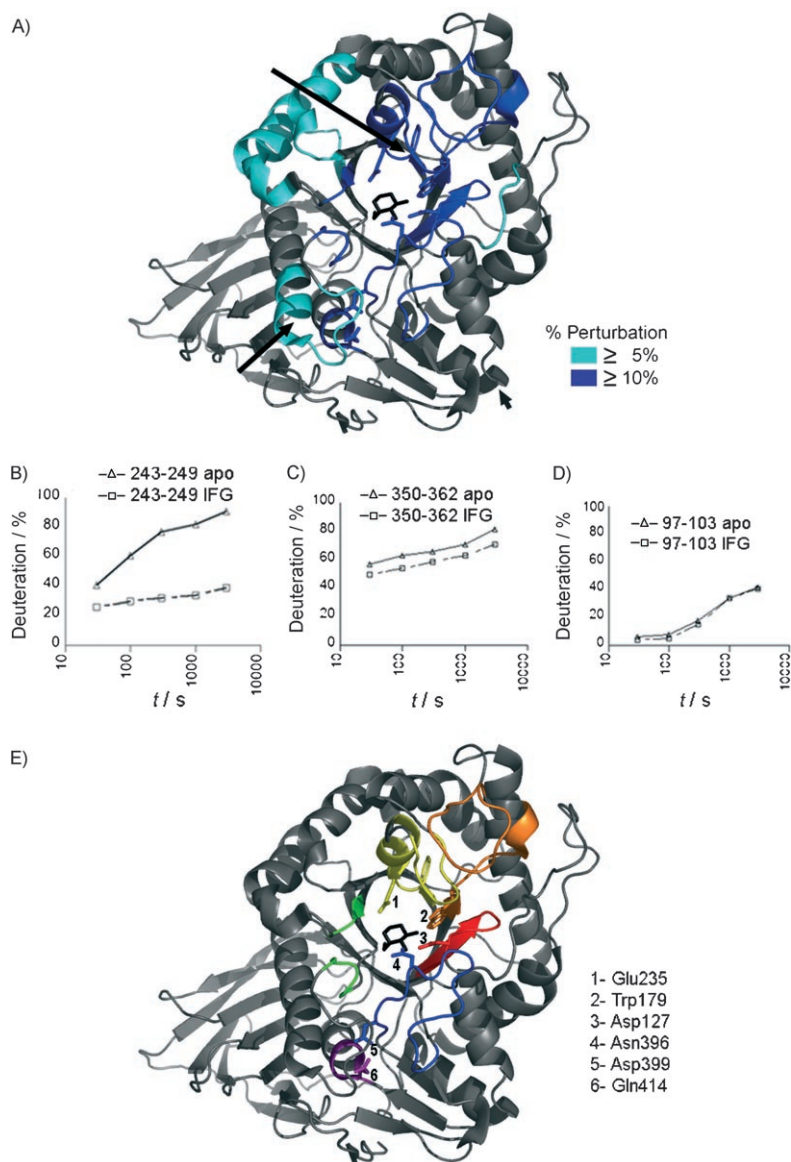


Figure 5. Isifogamine (IFG) induced perturbations in deuterium uptake upon binding to GCCase are superimposed upon the ribbon diagram representation of the IFG bound GCCase X-ray crystal structure (PDB ID: 2NSX). A) Highlighted are intermediate perturbations (5–8% decrease in average deuteriation level; cyan) and strong perturbations ($\geq 9\%$ decrease in average deuteriation level; blue). Illustrated are deuterium build-up curves representing B) a large perturbation (segment 243–249), C) an intermediate perturbation (segment 350–362) and D) no perturbation (segment 97–103). Intermediate perturbations correspond to the following segments: 130–134, 284–296, 315–336 ($\alpha 6$), and 350–362. Illustration generated with PyMOL (DeLano Scientific) and Kaleidagraph (Synergy Software). E) IFG rigidified regions with perturbations in $\geq 9\%$ are segments 119–127 (red), 177–184 (orange), 187–197 (orange), 230–240 (yellow), 243–249 (yellow), 310–312 (green), 343–347 (green), 386–400 (blue) and 414–417 (purple). IFG hydrogen bonded residues are labeled (Asp127, Trp179, Glu235 and Asn396). Also labeled are residues Asp399 and Gln414 which are likely hydrogen bonded.

nected to segment 310–312 ($\beta 6$) and is also adjacent to 284–296. Whereas segment 350–362 ($\alpha 7$) is sequentially adjacent to segment 343–347, it is conformationally adjacent to segment 414–417 ($\alpha 8$), a region that appears to undergo a propagated stabilization upon IFG binding through hydrogen bonding with segment 386–400. These regions are either sequentially

or conformationally adjacent to regions more closely associated with the active site or active site loop regions.

Discussion

DSF was employed to probe to what extent IFG imparted greater global stability. IFG was found to positively shift the transition midpoint of the heat denaturation curve by nearly 15°C (Figure 1A). Thus, it appears that a reduction in local unfolding properties of active site and active site loop regions translated into a gain in global stability.

It is now well established that IFG can enhance the activity of GCCase in N370S and G202R patient fibroblasts.^[7,8] Previous metabolic labeling experiments clearly illustrated that IFG facilitated the folding and transport of newly synthesized N370S GCCase out of the ER and into lysosomes.^[8] Furthermore, IFG increased the lysosomal pool of N370S GCCase isolated by Percoll gradient centrifugation.^[8] It can therefore be concluded that IFG is capable of gaining access to the ER luminal space, where it presumably imposes greater global stability upon mutant GCCase. Here we tested whether IFG is capable of stabilizing another GCCase mutant, F213I. IFG treatment produced a 4.3-fold enhancement in GCCase activity over non-treated F213I/L444P patient fibroblasts, demonstrating that this enhancement is not limited to the N370S and G202R mutations. A GD cell line homozygous for the L444P mutation did not respond to treatment with IFG (data not shown).

While X-ray crystallography can provide the fine details of a protein-ligand interaction, the structure is a static picture of the conformational space sampled by the protein. The Lieberman et al.^[7] crystallographic structure of the GCCase-IFG complex revealed a detailed network of hydrogen bonding interactions between GCCase and IFG. However, it is not clear how these interactions translate into increased global stability, resulting in enhanced protein folding, intercellular transport and lysosomal enzyme activity. Thus, additional information on changes that occur to protein dynamics upon ligand binding is needed to better understand the mechanism that ultimately produces these results.

Amide hydrogen exchange is a good descriptor of protein dynamics. A slow amide hydrogen exchange reaction indicates a less dynamic and more stable environment for the amide.^[24,33,34] Amide H/D exchange rate determination down to a resolution of six to ten amino acids has been made possible by combining proteolysis with mass spectrometry. This approach has been applied to probe the mechanism by which the hydrogen bonding network introduced by IFG binding is propagated throughout the folded GCCase molecule. To the best of our knowledge, this is the first time H/D-Ex has been used to directly monitor the ef-

fects of a PC on the molecular dynamics of specific regions of a lysosomal enzyme such as GCCase.

H/D-Ex results revealed that the effects of IFG binding propagate beyond the GCCase regions which are in direct contact with IFG. Whereas strong perturbations in the H/D exchange rate were observed in regions previously identified as directly hydrogen bound to IFG (segments 119–127, 177–184, 230–240, and 386–400), as well as others very close to these regions (segments 187–197, 243–249, 310–312, 343–347 and 414–417), weaker yet significant perturbations were observed in regions of the protein more distal from the active site (segments 130–134, 284–296, 315–336, and 350–362; see Figures 4 and 5). Since Lieberman et al.^[7] demonstrated no significant structural changes in GCCase upon IFG-binding (not including "loop 1"), H/D exchange rate perturbations observed outside of the active site could not have arisen through allostereism. Instead, the various breathing motions of the protein, both local and global fluctuations, appear to be restricted upon IFG binding.

H/D-Ex in combination with molecular dynamics simulations could be used to help elucidate the mechanism by which the binding of a PC translates into the stabilization of the target protein. H/D-Ex serves as an important adjunct to the techniques and considerations involved in optimizing the pharmacokinetics of a lead PC. These results also form the basis for future experiments involving protein dynamic comparisons of GCCase mutants, such as N370S and F213I, in the presence and absence of isofagomine or other PCs.

Experimental Section

Chemical reagents: Cerezyme (Imiglucerase) was purchased from Genzyme Corporation (Cambridge, MA). Isofagomine (IFG) was purchased from Toronto Research Chemicals (North York, Canada) and NanoOrange from Invitrogen. Fluorogenic substrates 4-methylumbelliferyl beta-D-glucopyranoside (MUGlc) and 4-methylumbelliferyl beta-N-acetylglucosaminide (MUG) were purchased from Sigma-Aldrich. All other reagents unless otherwise noted were obtained from Sigma-Aldrich.

Cell lines: Type I GD fibroblast cell lines harboring N370S/N370S and F213I/L444P mutations were kindly provided by Dr. Joe T.R. Clarke of the Sick Children's Hospital, Toronto (Canada) and Dr. F. Choy, University of Victoria (Canada), respectively. The first of two provided cell lines harbors a homozygous N370S substitution in the GCCase gene, GBA. The second cell line harbors one allele encoding a F213I substitution and its pair, a L444P substitution.

H/D-Ex experiments: The H/D-Ex protocol utilized in this experiment was previously elaborated upon in greater detail.^[27] Specific to this study, a GCCase stock solution in the presence or absence of IFG (59:1 molar ratio IFG to GCCase) was prepared by combining GCCase (50 μ L, 80 μ M in H₂O) with DMSO (5 μ L) containing IFG (47 mM) or with DMSO alone (5 μ L). An exchange reaction was initiated by diluting each mixture (5 μ L) with deuterated buffer (15 μ L, 50 mM Tris, pH 8.0). The reaction was allowed to proceed at 23 °C for a series of predetermined time periods (30, 100, 300, 1000 and 3000 s). Then the ex-

change reaction was quenched by lowering the temperature to 1 °C and the pH to 2.5 by the addition of a prechilled solution (1 °C; 30 μ L) containing 2 M urea and 1 M tris(2-carboxyethyl)phosphine hydrochloride (TCEP). The quenched solution was immediately pumped at 200 μ L min⁻¹ over an immobilized porcine pepsin column (104 μ L bed volume) with trifluoroacetic acid (TFA, 0.05%) for three minutes with contemporaneous collection of proteolytic products by way of a trap column (4 μ L bed volume). Pepsin was immobilized on Poros 20 AL media (30 mg mL⁻¹, Applied Biosystems) as per the manufacturer's instructions.^[27] Peptide fragments were eluted from the trap column and separated by C18 column (Magic C18, Michrom BioResources, Inc., Auburn, CA, USA) with a linear gradient of 13% solvent B to 40% solvent B over 23 min (solvent A, 0.05% TFA in water; solvent B, 95% acetonitrile, 5% water, 0.0025% TFA; flow rate changed from 10 μ L min⁻¹ at 0 min to 5 μ L min⁻¹ at 23 min). Mass spectrometric analyses were carried out with a Thermo Finnigan LCQTM mass spectrometer (Thermo Fisher Scientific, San Jose, CA) with a capillary temperature of 200 °C. Spectral data was acquired in data-dependent MS/MS mode with dynamic exclusion. The software program SEQUEST (Thermo Fisher Scientific, San Jose, CA) was used to tentatively identify the sequence of dynamically selected parent peptide ions. This tentative peptide identification was verified by visual confirmation of the parent ion charge state. These peptides were then further examined to determine if the quality of the measured isotopic envelope was of sufficient quality to allow an accurate geometric centroid determination. Centroid values were then determined using a proprietary program developed in collaboration with Sierra Analytics (Modesto, CA, USA). Back exchange corrections and deuteration level calculations were implemented as previously described elsewhere.^[28,35] Average per residue deuteration level calculations were weighted by the number of residues in each deuterated segment.

Differential scanning fluorimetry: GCCase (Cerezyme) suspension in water (30 mg mL⁻¹) was diluted in citrate phosphate (CP) buffer (10 mM citrate, 20 mM phosphate, pH 7.0) to 0.1 mg mL⁻¹. IFG was dissolved in DMSO to various concentrations (2.3 mM to 34 nM). IFG/NanoOrange mixtures were prepared by combining each diluted IFG stock with CP containing diluted enzyme (1 μ L of IFG stock plus 25 μ L diluted enzyme), followed by NanoOrange addition (25 μ L, 1:50 dilution of NanoOrange stock provided by manufacturer). A mock IFG/NanoOrange control was created by substituting DMSO (1 μ L) in lieu of the IFG stock. Mixtures were transferred to an Opticon Mini-cycler Real Time PCR machine (Bio-Rad CA, USA) and temperatures ramped from 30 to 90 °C over a period of 1 h. Fluorescence readings were recorded at 0.2 °C increments. The transition midpoint (T_m) of GCCase in the presence of different concentrations of IFG was calculated with the manufacturer's software.

Evaluation of the effect of IFG on GCCase activity in Gaucher patient cells: N370S/N370S or F213I/L444P patient fibroblasts were treated for 5 days with alpha-MEM media supplemented with FBS (10%) and containing IFG (25 μ M) or DMSO (1%). For

analysis of intracellular GCCase and hexosaminidase activity, media containing IFG or DMSO was removed, cells were rinsed twice with calcium- and magnesium-free PBS over a 5 min time period. Cells were trypsinized for 10–15 min at 37 °C, followed by centrifugation at 1000 rpm and washing with PBS. The final cell pellet was lysed by adding CP buffer (pH 5.5) containing Triton X-100 (0.4%) and taurodeoxycholate (0.4%). The lysate was cleared by centrifugation at 100 000 g and total soluble protein content determined using the Bradford Bio-Rad Protein Assay according to the manufacturers protocol (Bio-Rad). Enzymatic activity of both GCCase and β -hexosaminidase (Hex) was determined with the aid of artificial substrates MUGlc and MUG. Activity was measured by the increase in fluorescence due to release of the 4-methylumbelliferyl fluorophore from MUGlc and MUG. The increase in fluorescence was measured using a Spectramax M2 fluorometer (Molecular Devices Corp, Sunnyvale, CA), and detected at excitation and emission wavelengths set to 365 nm and 450 nm, respectively. Reactions were initiated by mixing equal volumes of lysate and substrate (0.8 mM MUGlc or 3.2 mM MUG) and then incubated at 37 °C for either 1 h (GCCase) or for 15 min (Hex). Reactions were terminated by raising the pH to 10.5, above the pK_a of 4-MU, with 0.1 M 2-amino-2-methyl-1-propanol. The effect of IFG on GCCase or Hex activity was determined by dividing the activity obtained in the presence of isofagomine by that obtained in the presence of DMSO only.

Acknowledgements

We gratefully acknowledge the funding partially provided by the CIHR Team Grant (2007) awarded to D.M. and M.B.T. and the technical assistance of Justin Buttner. Special thanks to F. Y. Choy at University Victoria (BC, Canada) for providing the GD patient fibroblast cell line F2131/L444P. We also gratefully acknowledge the Technology Fellowship program of New Jersey Commission on Science and Technology for providing funding in support of G.J.K.

Keywords: Gaucher disease · glucocerebrosidase · hydrogen/deuterium exchange · isofagomine · mass spectrometry · protein structures

- [1] S. U. Walkley, *Acta Paediatr. Suppl.* **2007**, *96*, 26.
- [2] Y. Kacher, A. H. Futerman, *FEBS Lett.* **2006**, *580*, 5510.
- [3] N. W. Barton, R. O. Brady, J. M. Dambrosia, A. M. Di Bisceglie, S. H. Doppelt, S. C. Hill, H. J. Mankin, G. J. Murray, R. I. Parker, C. E. Argoff, *N. Engl. J. Med.* **1991**, *324*, 1464.
- [4] G. M. Pastores, N. L. Barnett, E. H. Kolodny, *Clin. Ther.* **2005**, *27*, 1215.

- [5] D. Elstein, C. Hollak, J. M. Aerts, S. van Weely, M. Maas, T. M. Cox, R. H. Lachmann, M. Hrebicek, F. M. Platt, T. D. Butters, R. A. Dwek, A. Zimran, *J. Inherited Metab. Dis.* **2004**, *27*, 757.
- [6] J. Q. Fan, *Trends Pharmacol. Sci.* **2003**, *24*, 355.
- [7] R. L. Lieberman, B. A. Wustman, P. Huertas, A. C. Powe, Jr., C. W. Pine, R. Khanna, M. G. Schlossmacher, D. Ringe, G. A. Petsko, *Nat. Chem. Biol.* **2007**, *3*, 101.
- [8] R. A. Steet, S. Chung, B. Wustman, A. Powe, H. Do, S. A. Kornfeld, *Proc. Natl. Acad. Sci. USA* **2006**, *103*, 13813.
- [9] Z. Yu, A. R. Sawkar, L. J. Whalen, C. H. Wong, J. W. Kelly, *J. Med. Chem.* **2007**, *50*, 94.
- [10] V. Koprivica, D. L. Stone, J. K. Park, M. Callahan, A. Frisch, I. J. Cohen, N. Tayebi, E. Sidransky, *Am. J. Hum. Genet.* **2000**, *66*, 1777.
- [11] A. R. Sawkar, W. D'Haese, J. W. Kelly, *Cell. Mol. Life. Sci.* **2006**, *63*, 1179.
- [12] J. E. Bergmann, G. A. Grabowski, *Am. J. Hum. Genet.* **1989**, *44*, 741.
- [13] M. Schmitz, M. Alfalah, J. M. Aerts, H. Y. Naim, K. P. Zimmer, *Int. J. Biochem. Cell Biol.* **2005**, *37*, 2310.
- [14] L. Ellgaard, A. Helenius, *Nat. Rev. Mol. Cell Biol.* **2003**, *4*, 181.
- [15] L. Ellgaard, M. Molinari, A. Helenius, *Science* **1999**, *286*, 1882.
- [16] H. H. Chang, N. Asano, S. Ishii, Y. Ichikawa, J. Q. Fan, *FEBS J.* **2006**, *273*, 4082.
- [17] R. L. Wiseman, E. T. Powers, J. N. Buxbaum, J. W. Kelly, W. E. Balch, *Cell* **2007**, *131*, 809.
- [18] M. W. Pantoliano, E. C. Petrella, J. D. Kwasnoski, V. S. Lobanov, J. Myslik, E. Graf, T. Carver, E. Asel, B. A. Springer, P. Lane, F. R. Salemme, *J. Biomol. Screening* **2001**, *6*, 429.
- [19] N. Poklar, J. Lah, M. Salobir, P. Macek, G. Vesnaver, *Biochemistry* **1997**, *36*, 14345.
- [20] M. Vedadi, F. H. Niesen, A. Allali-Hassani, O. Y. Fedorov, P. J. Finerty, Jr., G. A. Wasney, R. Yeung, C. Arrowsmith, L. J. Ball, H. Berglund, R. Hui, B. D. Marsden, P. Nordlund, M. Sundstrom, J. Weigelt, A. M. Edwards, *Proc. Natl. Acad. Sci. USA* **2006**, *103*, 15835.
- [21] D. Matulis, J. K. Kranz, F. R. Salemme, M. J. Todd, *Biochemistry* **2005**, *44*, 5258.
- [22] F. H. Niesen, H. Berglund, M. Vedadi, *Nat. Protoc.* **2007**, *2*, 2212.
- [23] T. E. Wales, J. R. Engen, *Mass Spectrom. Rev.* **2006**, *25*, 158.
- [24] S. W. Englander, L. Mayne, Y. Bai, T. R. Sosnick, *Protein Sci.* **1997**, *6*, 1101.
- [25] J. J. Englander, C. Del Mar, W. Li, S. W. Englander, J. S. Kim, D. D. Stranz, Y. Hamuro, V. L. Woods Jr., *Proc. Natl. Acad. Sci. USA* **2003**, *100*, 7057.
- [26] S. W. Englander, *J. Am. Soc. Mass Spectrom.* **2006**, *17*, 1481.
- [27] Y. Hamuro, S. J. Coales, M. R. Southern, J. F. Nemeth-Cawley, D. D. Stranz, P. R. Griffin, *J. Biomol. Tech.* **2003**, *14*, 171.
- [28] Y. Hamuro, S. J. Coales, J. A. Morrow, K. S. Molnar, S. J. Tuske, M. R. Southern, P. R. Griffin, *Protein Sci.* **2006**, *15*, 1883.
- [29] A. P. Yeh, A. McMillan, M. H. Stowell, *Acta Crystallogr. Sect. D* **2006**, *62*, 451.
- [30] E. Beutler, W. Kuhl, F. Trinidad, R. Teplitz, H. Nadler, *Lancet* **1970**, *296*, 369.
- [31] A. R. Sawkar, W. C. Cheng, E. Beutler, C. H. Wong, W. E. Balch, J. W. Kelly, *Proc. Natl. Acad. Sci. USA* **2002**, *99*, 15428.
- [32] Y. Hamuro, S. J. Coales, K. S. Molnar, S. J. Tuske, J. A. Morrow, *Rapid Commun. Mass Spectrom.* **2008**, *22*, 1041.
- [33] A. Hvidt, S. O. Nielsen, *Adv. Protein Chem.* **1966**, *21*, 287.
- [34] S. L. Mayo, R. L. Baldwin, *Science* **1993**, *262*, 873.
- [35] Z. Zhang, D. L. Smith, *Protein Sci.* **1993**, *2*, 522.

Received: April 12, 2008

Published online on October 17, 2008